JCB Article

Rootletin, a novel coiled-coil protein, is a structural component of the ciliary rootlet

Jun Yang, Xiaoqing Liu, Guohua Yue, Michael Adamian, Oleg Bulgakov, and Tiansen Li

The Berman-Gund Laboratory for the Study of Retinal Degenerations, Harvard Medical School, Massachusetts Eye and Ear Infirmary, Boston, MA 02114

The ciliary rootlet, first recognized over a century ago, is a prominent structure originating from the basal body at the proximal end of a cilium. Despite being the largest cytoskeleton, its structural composition has remained unknown. Here, we report a novel 220-kD protein, designated rootletin, found in the rootlets of ciliated cells. Recombinant rootletin forms detergent-insoluble filaments radiating from the centrioles and resembling rootlets found in vivo. An mAb widely used as a marker for vertebrate rootlets recognizes an epitope in rootletin. Rootletin has a globular head domain and a tail domain consisting of extended coiled-coil structures. Rootletin forms parallel in register homodimers and elongated higher order polymers mediated by the tail domain alone. The head domain may be required for targeting to the basal body and binding to a kinesin light chain. In retinal photoreceptors where rootlets appear particularly robust, rootlets extend from the basal bodies to the synaptic terminals and anchor ER membranes along their length. Our data indicate that rootlets are composed of homopolymeric rootletin protofilaments bundled into variably shaped thick filaments. Thus, rootletin is the long-sought structural component of the ciliary rootlet.

Introduction

The ciliary rootlet as an anatomical structure was first discovered in 1880 (Engelmann, 1880), and its physical connection with the cilium and the basal body was recognized soon afterwards (Nussbaum, 1887). With the advent of electron microscopy, ultrastructural details of the rootlet were described for the first time in the 1950s (Sjostrand, 1953; Worley et al., 1953; Fawcett and Porter, 1954). The rootlet is a cytoskeleton-like structure, originating from the basal body and extending proximally toward the cell nucleus. Basal bodies are cellular organelles analogous to centrioles; in their role to nucleate the formation of cilia, centrioles are referred to as basal bodies. The invariable association of rootlets with basal bodies indicates that the latter structure also nucleates the formation of rootlets. The rootlets are typically seen as 80–100 nm in diameter, making them the largest cytoskeleton. Distinct cross striae are distributed at regular intervals of ~55–70 nm. In typical epithelial cells, rootlets can be traced down to the level of the nuclei, where they end without any special relationship to the nuclear membrane. The proximal portion of rootlets is extensively cross-linked to intermediate filaments (Lemullois et al., 1987).

A number of functions have been ascribed to the rootlets. Their cytoskeletal nature and the cross-linking between the rootlets and other cytoskeletons indicate an important role as an anchor and support structure for the cilia. Rootlets are associated with both motile and immotile cilia, the latter including the connecting cilia of vertebrate photoreceptor cells (Tokuyasu and Yamada, 1959; Cohen, 1960, 1965). In mammalian photoreceptors, the rootlets are very prominent and span much of the cells' lengths (Spira and Milman, 1979). The connecting cilia may be particularly dependent on rootlets for support, being a thin bridge linking the cell body and a comparatively giant organelle, the light-sensing outer segment (Besharse and Horst, 1990). Interaction between photoreceptor rootlets with membrane-bound vesicles, ER, Golgi, and mitochondria has been reported (Spira and Milman, 1979; Wolfrum, 1992), indicating a role in the proper positioning or anchoring of cellular organelles. A role for rootlets in intracellular protein transport has also been suggested (Fariss et al., 1997).

Though these proposals seem plausible, a definitive determination of the in vivo rootlet function requires knowledge of its structural constituent and the ability to manipulate it genetically. The question of what constitutes the ciliary rootlets in higher eukaryotes has remained unresolved despite numerous investigations. For example, centrin has been found in the

Address correspondence to Tiansen Li, Massachusetts Eye and Ear Infirmary, 243 Charles St., Boston, MA 02114. Tel.: (617) 573-3904. Fax: (617) 573-3216. E-mail: tli@meei.harvard.edu

*Abbreviations used in this paper: KLC3, kinesin light chain 3; SF-assemblin, striated fiber assemblin.

Key words: photoreceptor; cilium; striated fiber; basal body; centriole

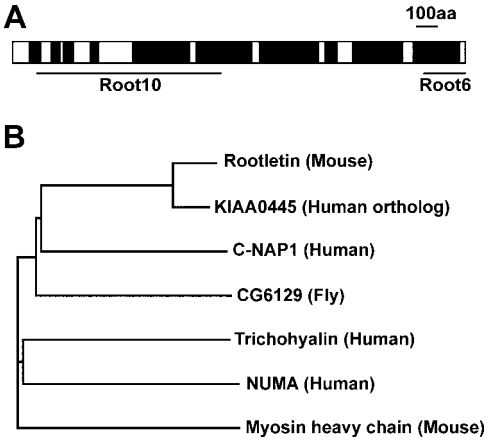

Figure 1. **Primary structure of mouse rootletin.** (A) Rootletin is predicted to form extended coiled-coil structures (filled blocks). The two horizontal lines underneath the structure diagram denote the regions used as antigens to produce antibodies (Root10 and Root6). (B) Phylogenetic tree of rootletin and related proteins. The phylogenetic tree was plotted using PAUP4.0. The sequences used were NP_055490 (KIAA0445), NP_009117 (C-NAP1), AAF56238 (CG6129), AAA65582 (Trichohyalin), XP_006005 (NUMA), and 008638 (Myosin heavy chain). The sequence data of rootletin are available from GenBank/EMBL/DDBJ under accession no. AF527975.

flagellar rootlets of green algae (Salisbury, 1995), but is not present in the ciliary rootlets of vertebrate photoreceptors (Wolfrum, 1995). Antigenic epitopes in rootlet-associated proteins have been documented using mAbs raised against partially purified rootlet preparations. An mAb (Clone CC310) recognizes a 175-kD protein associated with the rootlets in the chick oviduct (Klotz et al., 1986). This antibody recognizes ciliary rootlets in a variety of species, including mammals. Using a similar approach, a 195-kD protein was found in the rootlets of human oviduct epithelium (Hagiwara et al., 2000). Although these antibodies have been useful as markers for the rootlets, the identities of proteins that they recognize remain unknown. In the present work, we characterized a novel coiled-coil protein present in the ciliary rootlet. Our data suggest that this protein, which we have named rootletin, is a structural component of the rootlet. We propose that the ciliary rootlet is composed of homopolymeric protofilaments of rootletin.

Results

Identification of rootletin

Our initial encounter with rootletin was serendipitous. While characterizing antibodies against unrelated proteins, we noticed that some batches of antibody weakly stained mouse photoreceptor rootlets. We reasoned that if the fraction of antibody binding to rootlet could be enriched, it might be a useful tool for deciphering the composition of the rootlet. After extensive fractionation, we obtained an antibody preparation that recognized a single 220-kD protein from retinal homogenate and stained photoreceptor rootlets by immunocytochemistry. Screens of mouse retinal expression library with this antibody identified overlapping cDNA clones derived from a novel gene. Combined with 5′ and 3′ rapid amplification of cDNA ends, the full-length cDNA was shown to be 6,539 bases in length. Search of genome databases showed that this cDNA was encoded within a 40-kb ge-

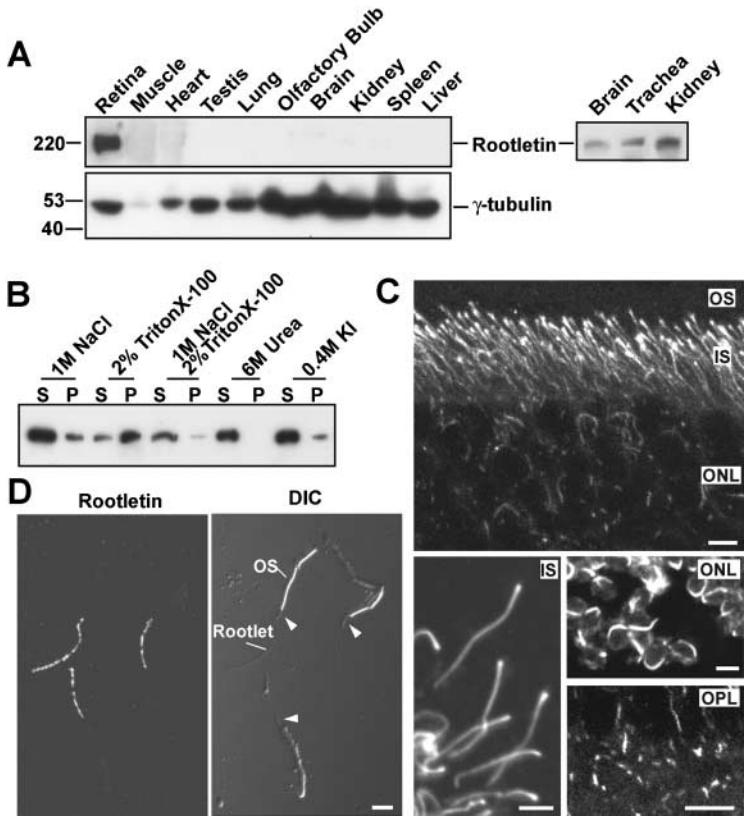

Figure 2. **Expression of rootletin in photoreceptor cells.** (A) Immunoblot analysis of multiple tissues. (Left) Rootletin antibodies detect a strong band at ~220 kD only in retina. Staining for γ-tubulin serves as a loading control. (Right) Weak rootletin bands are detected in brain, trachea, and kidney if sample loading is increased. (B) Rootletin is resistant to detergent extraction but is solubilized by high salt and by chaotropic and denaturing agents. S, supernatant; P, pellet. (C) Immunofluorescence of retinal sections indicates rootletin immunoreactivity spanning the inner segments (IS), curving around the nuclei (ONL), and terminating in the synaptic layer (OPL). Top: intact retina. Bottom: The sections were stained without fixation so the tissue was partially disrupted. This gave better staining signal and better illustration of rootletin distribution. (D) Immunostaining of dissociated photoreceptor cells. Rootletin antibodies stain only the rootlets attached at the base of the connecting cilia. This is illustrated by the matching Nomarski view (DIC) in which the outer segments, connecting cilia (arrowheads), and rootlets are visible. OS, outer segments; ONL, outer (photoreceptor) nuclear layer; OPL, outer plexiform (synaptic) layer. Bars, 5 μm.

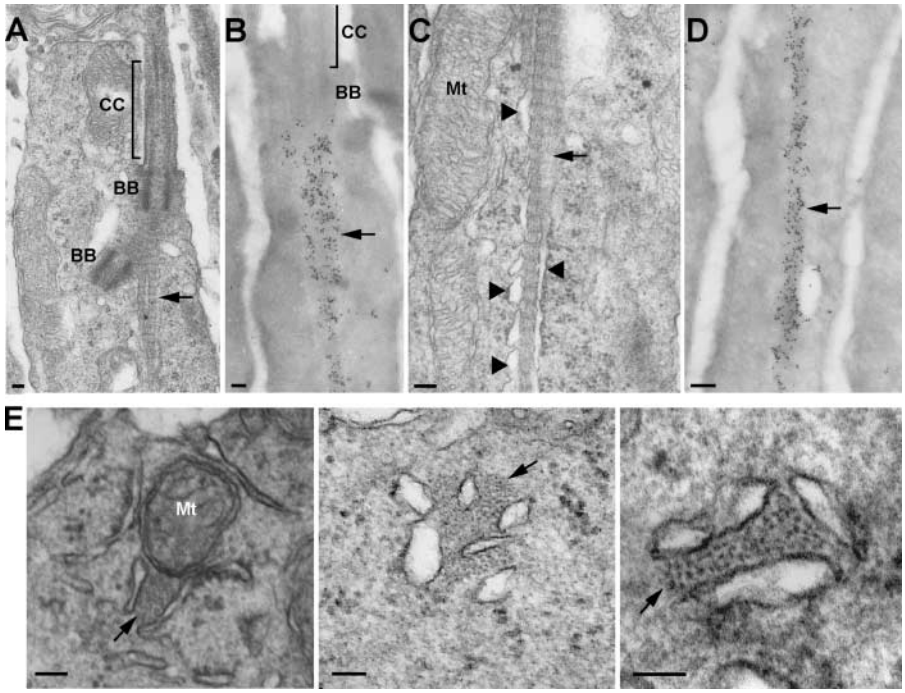

Figure 3. **Ultrastructural examination of the rootlets.** Images from plastic embedded sections (A, C, and E) and rootletin immunoreactivity on ultrathin cryosections (B and D) are shown. (A) A rootlet (arrow) originates from the basal body (BB) supporting the connecting cilium (CC) and extends proximally. A separate rootlet fiber connects the two basal bodies. (B) Rootletin is found only in the rootlet and not in the basal body or the connecting cilium. (C) A rootlet (arrow) coursing through the inner segment, with membranous saccules (arrowheads) in close juxtaposition. (D) Rootletin immunoreactivity is highly specific to the rootlet. (E) Transverse views of the rootlets at the level of ellipsoid inner segment. Rootlets are composed of bundles of 9–10-nm protofilaments (arrows). Rootlets are highly polymorphic and invariably surrounded by membranous compartments. Mitochondria (Mt) occasionally contact rootlets as well. Bars, 0.1 μm.

nomic region on mouse chromosome 4 (genome assembly no. GA_X5J8B7W862G; Celera). The full-length transcript is composed of 37 exons. The entire open-reading frame codes for a protein of 2,009 amino acid residues, which we subsequently designated rootletin. The conceptually translated polypeptide has a calculated molecular mass of 227 kD. Coils, Paircoil and Multicoil programs predict extended dimeric coiled coils (Lupas, 1996) in its COOH-terminal three quarters (Fig. 1 A). The NH_2-terminal one quarter of the primary sequence is likely to assume a globular structure.

Comparison with public protein databases indicates that rootletin is evolutionarily conserved (Fig. 1 B). The likely human orthologue of rootletin is an unknown protein (KIAA0445) encoded on human chromosome 1p36.11. A 6-kb region on the human X chromosome (GenBank/EMBL/DDBJ accession no. AL450472) is 80% identical to mouse rootletin. However, this sequence is intronless and presumably a pseudogene. The putative protein CG6129 appears to be the *Drosophila* orthologue of rootletin, with a similar domain organization and 48% similarity in amino acid sequence. Within the same mammalian species, the centrosomal protein C-Nap1 (Fry et al., 1998) is the only homologue of rootletin. Trichohyalin, NUMA, and myosin heavy chain are distantly related to rootletin, sharing sequence similarity only in the α-helical rod domain.

Rootletin is a component of the rootlet in all ciliated cells

To confirm that rootletin is indeed a component of the rootlet, two antibodies directed against different regions of mouse rootletin were generated (Fig. 1 A). Immunoblots using either Root10 or Root6 antibody revealed a polypeptide migrating at ~220 kD. Among multiple tissues examined, the retina exhibited the highest level of expression (Fig. 2 A). Smaller amounts of rootletin were detected in the brain, trachea, and kidney. Rootletin in the retina was primarily derived from photoreceptor cells because its level was greatly diminished in *rd* mouse retinas in which the photoreceptors had degenerated (unpublished data). Rootletin was found in the insoluble fraction of cell lysate. It was resistant to detergent extraction, but readily solubilized in high salt solutions, indicating ionic interaction is important in rootletin polymer formation. Rootletin was fully soluble in the presence of chaotropic agents or under denaturing conditions (Fig. 2 B).

By immunofluorescence, both rootletin antibodies recognized the photoreceptor rootlets, which appeared as prominent filamentous structures originating at the base of connecting cilia (Fig. 2 C). The rootlets continued through the photoreceptor nuclear layer, where they curved around the nuclei and terminated in a punctate pattern in the synaptic terminals. When photoreceptor cells were mechanically disrupted, the outer segments broke off from the cell body, usually with the connecting cilia and rootlets attached. Staining of this preparation demonstrated that rootletin was a stable component of the rootlets (Fig. 2 D).

By immunoelectron microscopy (Fig. 3, A–D), rootletin was found in the rootlet only and did not extend into the basal bodies. On cross sections (Fig. 3 E), rootlets were seen as bundles of individual thin filaments (protofilaments) with a diameter of 9–10 nm. The shape and dimension of the bundles were highly variable. Rootlets measured on cross sections were as wide as 300 nm or as narrow as 50 nm. The number of protofilaments in a bundle also varied widely. Interestingly, both longitudinal and cross-sectional views showed that rootlets were closely flanked by membranous saccules (Fig. 3, C and E). The saccules did not completely encircle the rootlet bundles; in some areas rootlets were exposed directly to the surrounding cytoplasm. The saccules were frequently seen continuous with rough ER, and their outer surfaces were also studded with ribosomes.

Immunostaining with rootletin antibodies found rootletin expression in all major ciliated epithelia (Fig. 4). Rootletin in ciliated epithelia lining the brain ventricles and tra-

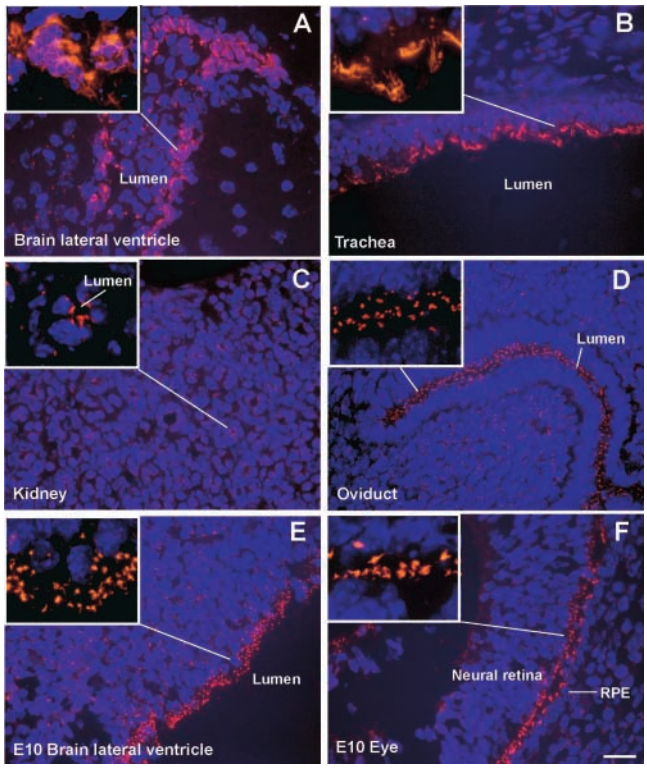

Figure 4. **Expression of rootletin in ciliated epithelia.** Rootletin immunostain (red); nuclear counter stain by Hoechst dye 33342 (blue). Insets show enlarged view. (A) Sagittal section through lateral ventricle of the brain (cells inside the lumen are in the choroid plexus). (B) Cross section of trachea. (C) Cortical region of the kidney sectioned through proximal and distal tubules. (D) Cross section of oviduct. (E and F) Sagittal sections of brain and eye from embryonic day-10 embryos. Bar, 20 μm.

chea appeared as a subapical meshwork originating from the cell cortex where basal bodies were aligned (Fig. 4, A and B). Fibrous materials extended proximally from the meshwork and wrapped around the nuclei. This staining pattern resembled the rootlet system in these cells described by previous ultrastructural studies. These observations suggest that rootletin is also a component of the rootlets in ciliated cells other than photoreceptors. By immunostaining, ciliated epithelia in brain and trachea exhibited highly developed rootlets. Rootlets in other types of cilia were less prominent. In the proximal and distal tubules of kidney (Fig. 4 C), rootlets appeared as relatively short and straight fibers. In the oviduct (Fig. 4 D), rootlets were rudimentary, appearing as large round spots. This is consistent with ultrastructural studies indicating lack of robust rootlets in mouse oviduct (Fawcett and Porter, 1954). Spermatids were devoid of rootletin-immunopositive fibers. During embryonic development, rootletin was enriched along the apical domains of neuroepithelium in the brain ventricular zone and the primordia of retinal pigment epithelium and the neural retina (Fig. 4, E and F), where rootletin was presumably associated with primary cilia.

In cells not known to develop cilia, rootletin immunostaining was seen as tiny speckles localized adjacent to the cell nuclei (Fig. 4 and Fig. 5 A). Double labeling for rootletin and γ-tubulin in COS cells showed that rootletin staining overlapped with centrioles (Fig. 5 A). On higher magnification, rootletin was seen to connect the proximal ends of the centriolar pair with a miniscule rootlet protruding away from the centrioles. These observations suggest that rootletin is present as a minute polymeric fibril at the centrioles of most (if not all) cells. Whether this indicates a potential centriolar function for rootletin or a leaky expression is entirely unknown. Rootletin staining disappears from the centrioles at the anaphase during mitosis (unpublished data).

If rootletin is the major structural component of the ciliary rootlet, recombinant expression of rootletin in heterologous cells should be sufficient to lead to rootlet formation. To test this hypothesis, we transiently expressed rootletin in COS cells. Expression of rootletin alone was sufficient to form detergent-insoluble thick filaments radiating from the centrosomal region (Fig. 5, A and B). Recombinant rootletin polymers formed in COS cells resembled rootlets in ciliated epithelia (Fig. 5 C). Ultrastructurally, rootletin polymers displayed the characteristic cross striae of rootlets seen in vivo (Fig. 5 D). The periodicity of these striae was ~60 nm, in line with the endogenous rootlets. A previously described mAb (CC310) is a widely used marker for the ciliary rootlets in a variety of animal species and cell types (Klotz et al., 1986). The rootlets assembled from recombinant rootletin were stained specifically by CC310 (Fig. 5 E). Thus, the CC310 antibody recognizes an epitope present in rootletin. Together, these data support the notion that rootletin is a major structural component of the rootlets in all ciliated cells.

Formation of rootlet from rootletin monomers

To examine how rootlets were formed from rootletin monomers, we analyzed a series of deletion constructs by protein interaction assays and by transient expression in COS cells. Deletion constructs of rootletin are schematically shown in Fig. 6 A. Four of them (R1, R2, R3, and R4) were tested for protein interactions in yeast two-hybrid assays. In these assays, each fragment was inserted into both a bait and a prey vector, and the bait and prey plasmids were cotransformed into yeast. Protein interactions were indicated by the rescue of nutritional markers in the cotransformants. The results are summarized in Fig. 6 B. The globular domain (R1) did not interact with any part of rootletin. In contrast, fragments derived from the rod domain (R2, R3, and R4) exhibited homotypic binding. In large-scale two-hybrid library screens, baits R3 and R4 also identified rootletin as an interacting partner, demonstrating the specificity of the interactions. These data indicate that the rod domain of rootletin mediates the formation of homodimers. Because each fragment binds only to itself, the rootletin dimer should be parallel and in axial register.

When transiently expressed in COS cells (Fig. 6 C), R1–R4 fragments did not form elongated fibers. R1 appeared as tiny speckles and congregated at the microtubule organizing center. R2–R4 fragments appeared as large dots encircling the nuclei. R123, which carries a deletion of 325 residues at the COOH terminus, also failed to form elongated filaments. R234, devoid of the globular domain but retaining the entire rod domain, remained competent to form elongated filaments. The filamentous network formed from R234 was ro-

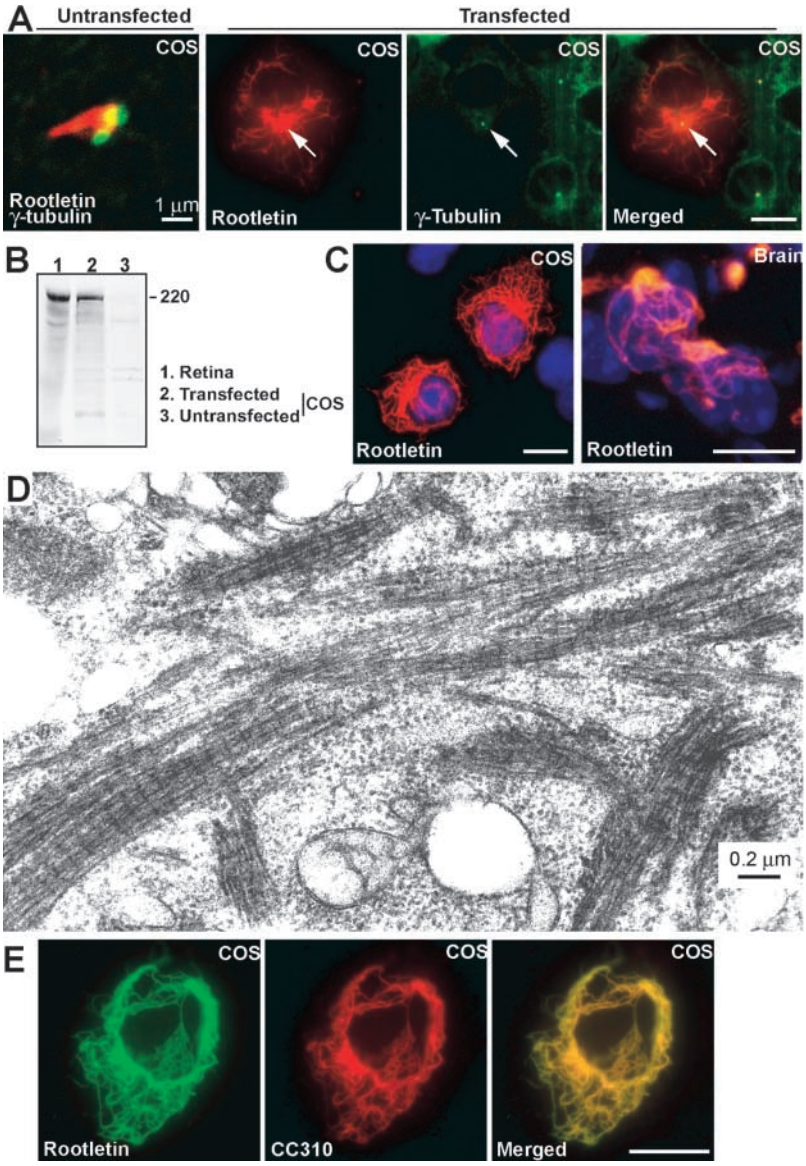

Figure 5. **Recombinant rootletin forms rootlet-like filaments in COS cells.** (A) In untransfected cells, endogenous rootletin (red) connects a pair of centrioles (revealed by the γ-tubulin staining [green]). Transient expression of recombinant rootletin results in the formation of a filamentous network (red) radiating from the centrioles (arrow). (B) Western blot confirms that the recombinant rootletin has the expected molecular mass (~220 kD). (C) Recombinant rootletin network (red) closely resembles that in epithelial cells lining brain ventricles. Nuclear counter stain by Hoechst dye 33342 (blue). (D) By electron microscopy, recombinant rootletin polymers exhibit the characteristic cross striae of native rootlets. (E) The mAb CC310, which recognizes a conserved epitope in vertebrate rootlets, stains recombinant rootletin. Bars, 15 μm unless otherwise noted.

bust, but did not appear to radiate from the microtubule organizing center. These data indicate that formation of higher order polymers is also mediated through interactions in the rod domain. The globular domain is not required for the formation of higher order polymers, but might have a role in targeting rootletin to centrioles/basal bodies.

Because the rod domain of rootletin exhibits homotypic binding, it is likely that truncated or otherwise mutated versions of rootletin will still interact with the full-length rootletin. As such, they may interfere with rootlet formation. To test this hypothesis, we cotransfected each of the rod domain fragments (R2, R3, and R4) in combination with the full-length rootletin. As shown in Fig. 6 D, each induced aggregates containing both the truncated and full-length rootletin, and inhibited formation of rootlets. These data suggest that certain mutant forms of rootletin readily incorporate with the normal rootletin and may act as strong dominant-negatives.

Although recombinant rootletin forms homopolymeric fibers resembling rootlets, rootlets in vivo may in fact be formed as a copolymer with an unidentified but homologous protein. To search for proteins that might copolymerize with rootletin, we performed immunoprecipitation of retinal homogenate and examined if another protein coprecipitated stoichiometrically with rootletin. On Coomasie dye staining, one visible polypeptide (excluding the immunoglobulin heavy and light chains) migrated at ~220 kD and was confirmed to be rootletin by immunoblotting (Fig. 6 E). The only mammalian homologue of rootletin is C-Nap1, which migrates at >250 kD. A protein of this size was not present in the immunoprecipitate. Together, the available data suggest that rootlets in vivo are composed of homopolymers of rootletin.

The globular head domain of rootletin interacts with kinesin light chain 3

The head domain of rootletin does not contribute to the formation of the rootletin filaments, indicating that this domain may protrude from the fibrous polymer and potentially interact with other proteins. To search for interacting partners, we performed yeast two-hybrid screening of a

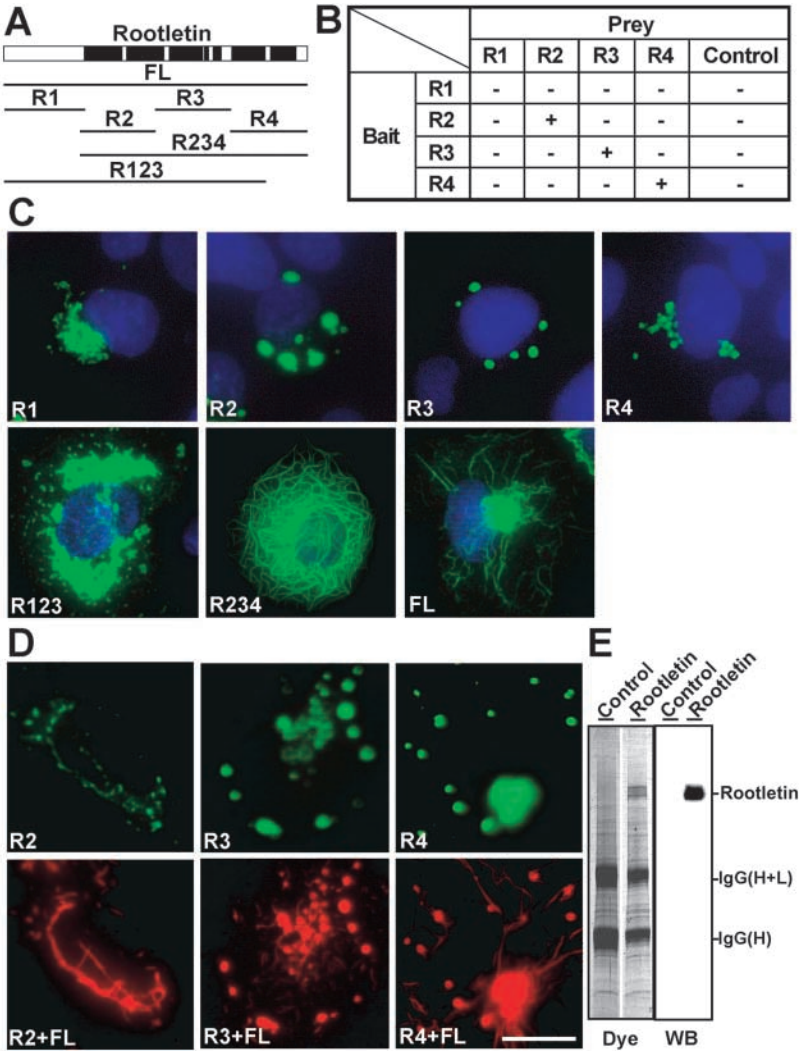

Figure 6. **Formation of rootlets from rootletin monomers.** (A) Schematic diagram of rootletin deletion constructs. (B) Yeast two-hybrid assays show homotypic binding between rootletin fragments derived from the rod domain. (+) interaction; (−) no interaction; (control) SV40 large T antigen. (C) Expression of rootletin constructs in COS cells shows only the full length (FL) rootletin and the intact rod domain (R234) are able to form elongated polymers. Rootletin or its fragments (green). Cell nuclei (blue). (D) Rootletin fragments derived from the rod domain (R2, R3, and R4) readily copolymerize with full length rootletin and disrupt rootlet formation. Rootletin fragments revealed by an EGFP tag (green). Rootletin antibody staining revealing the full length rootletin (as well as some of the fragments [red]). (E) Immunoprecipitation of retinal homogenate with rabbit Root10 antibody obtained a major protein migrating at ~220 kD (dye, Coomasie staining) that was confirmed to be rootletin (WB, Western blot). IgG H, IgG heavy chain; IgG H + L, undissociated heavy and light chains. Bar, 15 μm.

mouse retinal cDNA library using the head domain (R1) as a bait. 13 independent clones were identified from a screen of over 10^6 cotransformants that encoded the full-length cDNA for kinesin light chain 3 (KLC3),* a protein initially found in spermatids (Junco et al., 2001). To confirm the physical interaction between these two proteins, KLC3 was expressed either singly or in combination with the full-length rootletin in COS cells. When expressed alone, KLC3 fusion protein appeared as amorphous aggregates in COS cells (Fig. 7 A). Coexpression with rootletin lead to distribu-

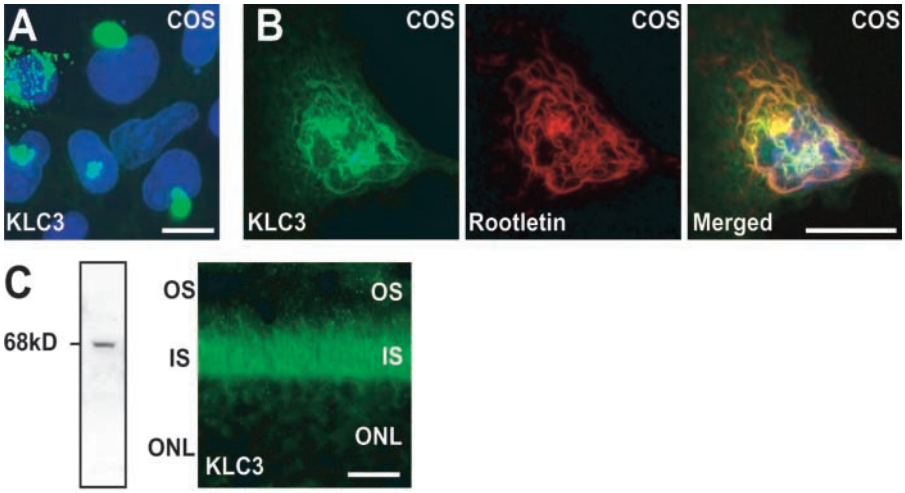

Figure 7. **Interaction of rootletin with KLC3.** (A) Transiently expressed KLC3 (green) appears as aggregates surrounding the nuclei (blue). (B) KLC3 distributes along the rootletin fibers upon cotransfection of rootletin (red) and KLC3 (green) into COS cells. (C) KLC3 is abundantly expressed in the retinal photoreceptors. KLC3 appears as a single band on immunoblot of retinal homogenate with a molecular mass of ~68 kD (left). Immunostaining of retina sections shows KLC3 in the inner segments of photoreceptors (right). OS, outer segment; IS, inner segment; ONL, outer (photoreceptor) nuclear layer. Bars, 15 μm.

tion of KLC3 along the rootlet fibers (Fig. 7 B). These data confirm the physical interaction between KLC3 and rootletin. To investigate if KLC3 was present in photoreceptors, we conducted immunostaining and immunoblotting with KLC3 antibodies. KLC3 was detected as a single band on immunoblots from retinal homogenate and was abundant in the inner segments of photoreceptors (Fig. 7 C). Therefore, KLC3 is localized in the same subcellular compartment as rootletin in the photoreceptors. These data suggest that the interaction between KLC3 and rootletin could potentially be physiologically relevant.

The rootlet and other cytoskeletons

The rootlet is thought to be cross-linked and bundled with other cytoskeletons. A relationship between rootlets and other cytoskeletons would be difficult to investigate in mammalian photoreceptors because of their small size. Therefore, we performed studies in COS cells transiently expressing recombinant rootletin (Fig. 8). In interphase cells, recombinant rootlet formation mildly perturbed the microtubule network, causing increased microtubule bundling. The two cytoskeletal networks did not colocalize. Dissolution of microtubule network by treatment with nocodazole did not abolish the recombinant rootletin network. During mitotic spindle formation, microtubules were extensively reorganized, whereas the rootlet fibers remained intact. There appeared to be no colocalization between rootlets and the intermediate and actin filaments. These observations indicate that recombinant rootlets and other major cytoskeletal networks are not interdependent, extensively cross-linked, or coordinately regulated. Recombinant rootlets exhibited minimal colocalization with the ER and Golgi membranes. Thus, interaction with other cytoskeletons or anchoring of cellular organelles may be cell-type dependent; mediated through additional protein–protein interactions that are cell- or tissue-specific.

Discussion

In this paper, we demonstrate that the primary function of rootletin is to form the ciliary rootlet. The rootlet is found in diverse organisms across wide phylogenetic distances, from green algae, mollusks, amphibians, to mammals. Until now, no structural components of the rootlet in higher eukaryotes have been reported. The only known components of the rootlet have been found in green algae in which centrin and striated fiber assemblin (SF-assemblin) were shown to be components of the contractile and noncontractile rootlet fibers, respectively. Centrin, a calcium-binding protein related to calmodulin, is a ubiquitous 20-kD component of the centrosome. It is also a major component of the contractile fiber called the nucleus–basal body connector (Salisbury et al., 1984). SF-assemblin is the major structural component of the striated rootlet fibers. It is a 33-kD protein with a nonhelical head domain and an α-helical tail domain predicted to form a coiled-coil rod structure (Lechtreck and Melkonian, 1998). Recombinant expression of SF-assemblin alone leads to the formation of striated fibers. Although no sequence homology could be detected between the SF-assemblin and the mammalian rootletin, the two proteins may share similarities in how they are assembled into homopolymeric filaments. Our study suggests that rootletin is a major structural component of the rootlet in mammalian species. A putative protein in *Drosophila* (CG6129) has an overall similar structure to rootletin and appears to be the orthologue to the mammalian rootletin. If confirmed by future studies, it would suggest that a rootletin-like protein is used to construct the rootlet in most higher eukaryotic species.

Rootletin is predicted to form extended coiled-coil structures. Coiled-coil interactions produce stable polymers, as exemplified by intermediate filaments, collagen fibers, and the tail domain of myosin heavy chains, among others. Thus, coiled-coil interaction in the extended α-helical rod domain

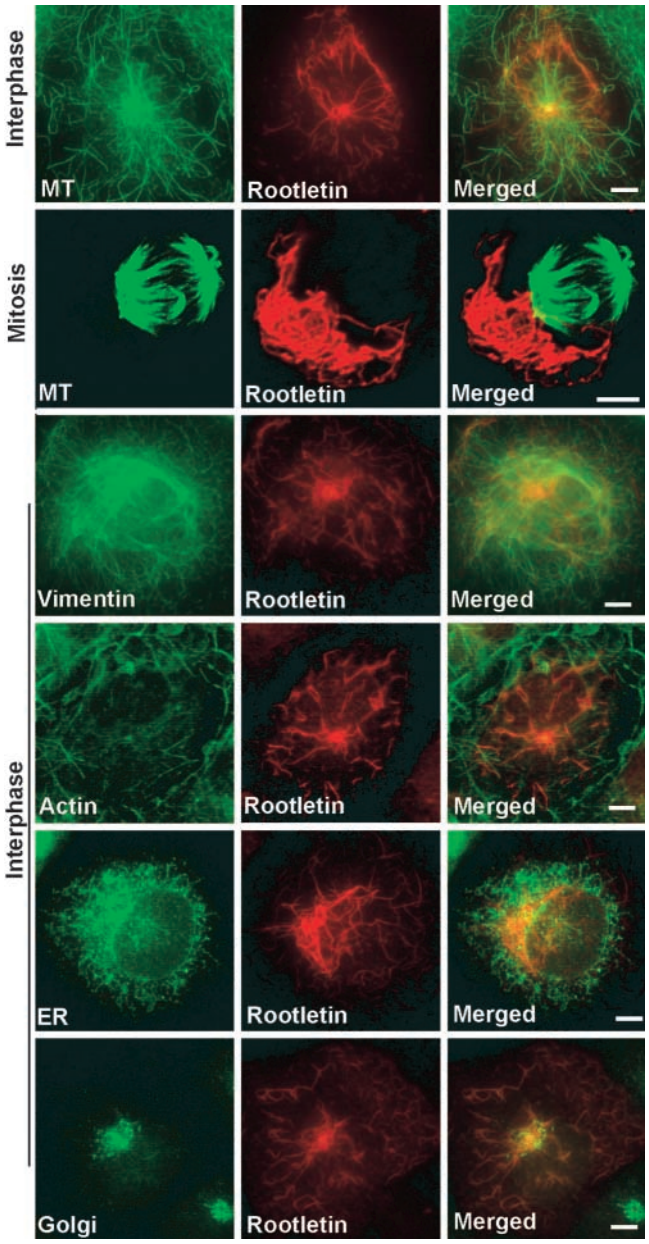

Figure 8. **Double labeling of rootlets (red) and other cytoskeleton or organelles (green) in COS cells, after transient expression of recombinant rootletin.** There is no extensive colocalization between recombinant rootlets and major cytoskeletal networks or organelles. Bars, 5 μm.

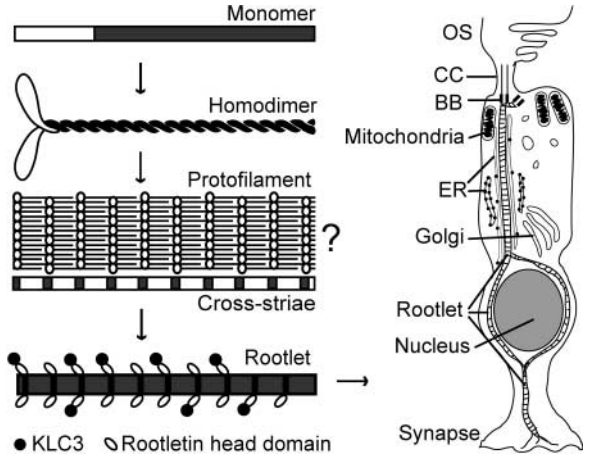

Figure 9. **Model for assembly of rootlet from rootletin monomers.** Filled segment of the monomer is predicted to form a coiled-coil structure. The homodimer is parallel and in axial register. The characteristic cross striation is likely the result of alternating protein-packing densities. KLC3 has been shown to interact physically with the head domain of rootletin, but a physiological relevance has not been established. A photoreceptor cell, in which the rootlet extends from the basal body to the synapse, is shown on the right. See Discussion for further details.

of rootletin is a key feature in rootlet formation. We propose a model to account for the assembly of rootlets from rootletin monomers (Fig. 9). The first step is the formation of rootletin homodimers that are parallel and in axial register. Formation of higher order elongated polymers does not require head-to-head or head-to-tail interactions because the globular head domain is dispensable. Instead, lateral binding within the rod domain of rootletin dimers, which primarily involves ionic interactions, is important. The resulting rootletin protofilament has a diameter of ~10 nm, similar to intermediate filaments. By analogy, the number of rootletin monomers in a cross section of the protofilament may be close to 32. The periodicity of cross striation likely corresponds to the axial stagger; the repeat segments of lower packing density incorporate more stain and manifest as darker (electron dense) bands. Finally, the rootlet itself is assembled from bundled rootletin protofilaments. These bundles are highly variable with respect to the shape and the number of protofilaments within, giving rise to variable appearance of rootlets. By morphological criteria, individual rootlet protofilament would be indistinguishable from intermediate filaments. Previous studies have suggested that in cells in which the rootlets are less developed, there tends to be a concomitant increase in the fibrous component of the apical cortex. These fibrous components may in fact be nonbundled rootlet protofilaments.

The model presents a simplified view of the elongated polymer, and many aspects remain uncertain. First, it is not yet clear whether the rootletin dimers are arranged in a parallel or an antiparallel configuration. Second, a rough estimate puts the length of the rod domain at ~200 nm, based on an axial rise per residue of 0.1485 nm. The mode of packing in the present model would suggest a periodicity of 100 nm. To reconcile with the observed periodicity of cross striae at 60–70 nm, additional complexity in packing is likely to be involved.

The globular head domain is found to physically interact with KLC3. Although originally characterized as a protein enriched in spermatids [Junco et al., 2001], our analysis shows that KLC3 is also abundant in photoreceptors. This interaction may have a role in transporting rootletin to the proximal basal body, where rootlet formation initially occurs. Alternatively, the rootlet may be associated with the kinesin motor complex and is involved in the trafficking of other proteins. In this regard, it is interesting to note that the rootlet has been suggested to play a role in the transport of a photoreceptor-specific protein (Fariss et al., 1997). A number of studies have also identified ATPase activity overlapping with the cross striation of the rootlet (Matsusaka, 1967), consistent with an association of rootletin with motor proteins. The physiological significance in the rootletin–KLC3 interaction remains to be established.

Our finding that rootletin normally localizes to the proximal ends of centrioles in nonciliated cells raises the possibility of a centriolar function for rootletin. In this putative role, a possible connection to the function of C-Nap1 is intriguing. Rootletin substantially overlaps with C-Nap1 in many molecular and cell biological aspects. The two proteins are similar in primary sequence and in overall domain organization. Both proteins are found at the centrioles and disassemble from the mitotic spindle at anaphase during mitosis. C-Nap1 is proposed to play a role in cell cycle-regulated centrosome cohesion, i.e., the linkage between the two centrioles. Yet, C-Nap1 is restricted to the proximal ends of individual centrioles and is therefore not the linker itself (Mayor et al., 2000). In contrast, striated rootlet fibers are seen linking the two basal bodies (Fig. 3 A). In nonciliated cells, rootletin polymers appear to overlap with the two centrioles (Fig. 5 A). Thus, rootletin appears able to fulfill the role of a centriolar linker. In this putative scenario, the linker is composed of rootletin polymers that may interact with C-Nap1 at the points of centriolar attachment.

Rootlets are associated with all types of cilia, be they motile, sensory, or primary. Our data suggest that both recessive null and dominant negative mutations of rootletin may disrupt the formation of rootlets. Clinical entities such as the immotile cilium syndrome, primary ciliary dyskinesia, and retinitis pigmentosa are candidates for having a genetic defect in rootletin. How such a deficit will in turn affect the structure and function of the cilia and the host cells will provide much insight into the physiological role of the rootlet. The rootlet is well known, yet still mysterious. Identification of rootletin as its structural component marks a major step forward toward understanding this organelle.

Materials and methods

Cloning rootletin

A pAb raised in chicken against a GST-fusion protein was found to cross-react with the ciliary rootlets of mouse photoreceptor cells. Fractionation of this antibody through affinity columns carrying different moieties of the fusion protein indicated that the GST-reactive fraction recognized the rootlets. The latter fraction was then used to screen an expression cDNA library made from C57BL/6 mouse retinal RNA in the λ phage vector Uni-Zap (Stratagene). Positive clones were analyzed by DNA sequencing. To obtain cDNA clones with full-length coding sequence, inserts from initial cDNA clones were used as probes in a second round of library screening by DNA hybridization. Putative full-length clones were confirmed by 5′

and 3′ rapid amplification of cDNA ends. RNA templates used for these assays were also derived from C57BL/6 mouse retinas.

Antibodies, immunofluorescence, immunoprecipitation, and immunoblotting

cDNA fragments coding for amino acid residues 101–923 (Root10) and 1819–2006 (Root6) of mouse rootletin were inserted into the expression vector pET28b (Novagen). Recombinant proteins were expressed as His-tagged fusion proteins in the *Escherichia coli* host BL21(DE3)pLysS. The recombinant proteins were purified through a Ni^{2+}-charged nitriloacetic acid agarose column and were used to immunize rabbits and chickens. Rootletin-specific antibodies were affinity-purified from antisera or egg yolk extracts. Different rootletin antibodies gave similar results on immunoblots and on immunofluorescence. Unless otherwise noted, data in this report were obtained using both rabbit anti-Root6 and anti-Root10 antibodies. MAb CC310 (Klotz et al., 1986) and anti-KLC3 pAb (Junco et al., 2001) were described previously. Monoclonal antiacetylated α-tubulin, monoclonal anti–γ-tubulin, monoclonal anti-Golgi58, polyclonal anti–actin, monoclonal anti–vimentin, and monoclonal anti–cytokeratin 7 antibodies were obtained from Sigma-Aldrich. Monoclonal anti-KDEL (ER marker) antibody was obtained from Calbiochem. Alexa 488– and Alexa 594–conjugated secondary antibodies were obtained from Molecular Probes, Inc.

Immunofluorescence and immunoblotting were performed essentially as described previously (Hong et al., 2001). Tissues were collected from normal mice (C57BL/6) after euthanasia by CO_2 inhalation. To prepare dissociated photoreceptors, retinas were dissected out and collected in a microcentrifuge tube containing 0.5 ml PBS. The tube was shaken vigorously for a few seconds and allowed to settle. The buffer containing broken photoreceptor cells was transferred onto glass slides (Superfrost Plus; Fisher Scientific International). Materials adhering to the glass slides contained many outer segments attached to the connecting cilia, rootlets, and sometimes remnants of inner segment membranes. They were fixed in 4% formaldehyde/PBS for 10 min before immunostaining. Cultured cells were fixed in a mixture of methanol–acetone at −20°C for 10 min before immunostaining. Cell nuclei were counterstained with Hoechst dye 33342. Slides were mounted in an aqueous mounting medium, viewed, and photographed on a fluorescent microscope (model IX70; Olympus) equipped with a digital camera (Carl Zeiss MicroImaging, Inc.) or on a confocal laser scanning microscope (model TCS SP2; Leica), using the AxioVision 2.0 software and the Leica Confocal Software, respectively.

To assess the solubility of rootletin, retinas were homogenized in a buffer containing 10 mM Tris, pH 7.5, 10 mM EGTA, 2 mM $MgCl_2$, 1 mM DTT and protease inhibitors. After a low speed centrifugation to remove nuclei, the supernatant was centrifuged at 170,000 *g* for 40 min. Pellets were then extracted at RT for 10 min in various buffers as shown in Fig. 2 B. The resulting supernatants and pellets were analyzed by immunoblotting.

For immunoprecipitation, mouse retinas were homogenized in a buffer containing 10 mM Tris, pH 7.4, 300 mM NaCl, 1 mM DTT and protease inhibitors. The homogenate was centrifuged at 18,000 *g* for 5 min. The supernatant was precleared by incubating with protein G agarose followed by centrifugation at 2,000 *g* for 2 min. The supernatant was incubated with either rabbit anti–Root10 antibody or nonimmune rabbit IgG, and then with protein G-agarose for 1 h each at RT. After washing, the bound materials were eluted by incubating with SDS protein sample buffer at 70°C for 20 min. Samples were separated by SDS-PAGE and analyzed either by staining with Coomasie dye or by immunoblotting using the chicken anti–Root6 antibody.

Transient expression of recombinant rootletin

COS-7 cells were maintained in DME supplemented with 5% FBS at 37°C in 5% CO_2. Transfection was performed using the Geneshuttle™-40 reagent (Qbiogene, Inc.) according to the manufacturer's instructions. To express rootletin or its fragments, the cDNAs were inserted into the mammalian expression vector pcDNA3.1(−) (Invitrogen) or pEGFP-C2 (CLONTECH Laboratories, Inc.). Cells were processed 30 h after transfection. Expression constructs used in the expression studies were as follows (the numbers denote amino acid residues): R1, 3–533; R2, 501–1000; R3, 999–1500; R4, 1495–2009; R123, 1–1684; R234, 501–2009; FL, 1–2009.

Electron microscopy and immunoelectron microscopy

For transmission electron microscopy, enucleated eyes were fixed for 10 min in 1% formaldehyde, and 2.5% glutaraldehyde in 0.1 M cacodylate buffer (pH 7.5). After removal of the anterior segments and lens, the eye cups were left in the same fixative at 4°C overnight. Eye cups were washed with buffer, post-fixed in osmium tetroxide, dehydrated through a graded alcohol series, and embedded in Epon. Sections were stained in uranyl acetate and lead citrate before viewing on an electron microscope (model 100CX; JEOL USA, Inc.). To examine ultrastructural localization of rootletin, mouse eyes were processed for immunoelectron microscopy as described previously (Hagstrom et al., 2001) and stained using the rabbit anti–rootletin Root6 antibodies. To examine the ultrastructure of recombinant rootletin polymers, the pEGFP-R234 expression construct was transiently expressed in COS-7 cells. In this construct, the head domain of rootletin dispensable for polymer formation was replaced by GFP for ease of tracking cells expressing the recombinant protein. Cells were treated with 20 μM nocodazole for 1.5 h before harvesting. Cells were scraped off the culture vessel, pelleted, and fixed for 1 h in a solution containing 0.5% saponin, 2% tannic acid, 1% formaldehyde, and 2.5% glutaraldehyde in 0.1 M cacodylate buffer (Maupin and Pollard, 1983). Cells were post-fixed in 1% osmium tetroxide, dehydrated through a graded alcohol series, and embedded in Epon. Sections were stained in uranyl acetate and lead citrate before viewing.

Yeast two-hybrid screening

Cloning vectors, yeast host cells, and reagents were purchased from CLONTECH Laboratories, Inc. A GAL4-based two-hybrid system (System 3) was used. A retinal cDNA library was constructed using poly$(A)^+$ RNA from C57BL/6 mouse retinas and inserted into the pACT2 plasmid vector. The bait plasmid was constructed by inserting a cDNA encoding the bait protein into the pGBKT7 plasmid vector. Library screening was performed according to the manufacturer's instructions. To test interactions directly, these fragments were also inserted into the prey vector pGADT7 and cotransformed with the bait plasmids into yeast host cells. Positive colonies were identified based on their ability to express nutritional markers HIS3 and ADE2 as well as a *lacZ* reporter. Each cotransformation experiment was plated out on both SD-4 (-Leu, -Trp, -Ade, and -His) and SD-2 (-Leu and -Trp) plates. The latter served as a control for successful cotransformation. A bait–prey combination was deemed interacting if the following criteria were met: (1) colonies were recovered from SD-4 plates; (2) colonies were completely white (indicating functioning adenine biosynthetic pathway); and (3) colonies turned blue upon exposure to α–X-Gal substrate (CLONTECH Laboratories, Inc.). Negative pairings yielded no colonies on SD-4 plates.

GenBank accession number

Mouse rootletin (GenBank/EMBL/DDBJ accession no. AF527975).

We thank Drs. D. Hong and Y. Zhao for helpful suggestions, and Drs. J. Aparicio (University of Southern California, Los Angeles, CA), F. van der Hoorn (University of Calgary, Alberta, Canada), and C. Klotz (Centre de Génetique Moléculaire du CNRS, Gifsur Yvette, France) for gifts of antibodies.

This work was supported by a National Institutes of Health grant (EY10309). T. Li is a Research to Prevent Blindness Sybil B. Harrington Scholar.

Submitted: 26 July 2002
Revised: 27 September 2002
Accepted: 27 September 2002

References

Besharse, J.C., and C.J. Horst. 1990. The photoreceptor connecting cilium: a model for the transition zone. *In* Ciliary and Flagellar Membranes. R.A. Bloodgood, editor. Plenum, New York. 389–417.

Cohen, A.I. 1960. The ultrastructure of the rods of the mouse retina. *Am. J. Anat.* 107:23–48.

Cohen, A.I. 1965. New details of the ultrastructure of the outer segments and ciliary connectives of the rods of human and macaque retinas. *Anat. Rec.* 152: 63–80.

Engelmann, T.W. 1880. Zur anatomie und physiologie der flimmerzellen. *Arch gel Physiol.* 23:505–535.

Fariss, R.N., R.S. Molday, S.K. Fisher, and B. Matsumoto. 1997. Evidence from normal and degenerating photoreceptors that two outer segment integral membrane proteins have separate transport pathways. *J. Comp. Neurol.* 387: 148–156.

Fawcett, D.W., and K.R. Porter. 1954. A study of the fine structure of ciliated epithelia. *J. Morphol.* 94:221–282.

Fry, A.M., T. Mayor, P. Meraldi, Y.D. Stierhof, K. Tanaka, and E.A. Nigg. 1998. C-Nap1, a novel centrosomal coiled-coil protein and candidate substrate of the cell cycle-regulated protein kinase Nek2. *J. Cell Biol.* 141:1563–1574.

Hagiwara, H., T. Aoki, N. Ohwada, and T. Fujimoto. 2000. Identification of a 195 kDa protein in the striated rootlet: its expression in ciliated and ciliogenic cells. *Cell Motil. Cytoskeleton.* 45:200–210.

Hagstrom, S.A., M. Adamian, M. Scimeca, B.S. Pawlyk, G. Yue, and T. Li. 2001. A role for the Tubby-like protein 1 in rhodopsin transport. *Invest. Ophthalmol. Vis. Sci.* 42:1955–1962.

Hong, D.H., G. Yue, M. Adamian, and T. Li. 2001. A retinitis pigmentosa GTPase regulator (RPGR)-interacting protein is stably associated with the photoreceptor ciliary axoneme and anchors RPGR to the connecting cilium. *J. Biol. Chem.* 276:12091–12099.

Junco, A., B. Bhullar, H.A. Tarnasky, and F.A. van der Hoorn. 2001. Kinesin light-chain KLC3 expression in testis is restricted to spermatids. *Biol. Reprod.* 64:1320–1330.

Klotz, C., M. Bordes, M.C. Laine, D. Sandoz, and M. Bornens. 1986. A protein of 175,000 daltons associated with striated rootlets in ciliated epithelia, as revealed by a monoclonal antibody. *Cell Motil. Cytoskeleton.* 6:56–67.

Lechtreck, K.F., and M. Melkonian. 1998. SF-assemblin, striated fibers, and segmented coiled coil proteins. *Cell Motil. Cytoskeleton.* 41:289–296.

Lemullois, M., P. Gounon, and D. Sandoz. 1987. Relationships between cytokeratin filaments and centriolar derivatives during ciliogenesis in the quail oviduct. *Biol. Cell.* 61:39–49.

Lupas, A. 1996. Coiled coils: new structures and new functions. *Trends Biochem. Sci.* 21:375–382.

Matsusaka, T. 1967. ATPase activity in the ciliary rootlet of human retinal rods. *J. Cell Biol.* 33:203–208.

Maupin, P., and T.D. Pollard. 1983. Improved preservation and staining of HeLa cell actin filaments, clathrin-coated membranes, and other cytoplasmic structures by tannic acid-glutaraldehyde-saponin fixation. *J. Cell Biol.* 96: 51–62.

Mayor, T., S. York-Dieter, K. Tanaka, A.M. Fry, and E.A. Nigg. 2000. The centrosomal protein C-Nap1 is required for cell cycle-regulated centrosome cohesion. *J. Cell Biol.* 151:837–846.

Nussbaum, M. 1887. Ueber die theilbarkeit der lebendegen materie. ii. Beitrage zur naturgeschichte des Genus Hydra. *Arch mikr Anat.* 29:265–366.

Salisbury, J.L. 1995. Centrin, centrosomes, and mitotic spindle poles. *Curr. Opin. Cell Biol.* 7:39–45.

Salisbury, J.L., A. Baron, B. Surek, and M. Melkonian. 1984. Striated flagellar roots: isolation and partial characterization of a calcium-modulated contractile organelle. *J. Cell Biol.* 99:962–970.

Sjostrand, F.S. 1953. The ultrastructure of the inner segments of the retinal rods of the guinea pig eye as revealed by electron microscopy. *J. Cell. Comp. Physiol.* 42:45–70.

Spira, A.W., and G.E. Milman. 1979. The structure and distribution of the cross-striated fibril and associated membranes in guinea pig photoreceptors. *Am. J. Anat.* 155:319–338.

Tokuyasu, K., and E. Yamada. 1959. The fine structure of the retina studied with the electron microscope. *J. Biophys. Biochem. Cytol.* 6:225–230.

Wolfrum, U. 1992. Cytoskeletal elements in arthropod sensilla and mammalian photoreceptors. *Biol. Cell.* 76:373–381.

Wolfrum, U. 1995. Centrin in the photoreceptor cells of mammalian retinae. *Cell Motil. Cytoskeleton.* 32:55–64.

Worley, L.G., E. Fischbein, and J.E. Shapiro. 1953. The structure of ciliated epithelial cells as revealed by the electron microscope and in phase contrast. *J. Morphol.* 92:545–577.